Materials Science and Engineering, 46 (1980) 129 - 144

Study of Intrinsic Point Defects in Tantalum after Plastic Deformation at Liquid Helium Temperatures

HOLLEMBERT
HERNÁN A. PERETTI, MANUEL A. MONDINO* and ALFRED SEEGER†

Centro Atómico Bariloche, Comisión Nacional de Energía Atomica; Instituto de Física "Dr. J. A. Balseiro", Universidad Nacional de Cuyo, 8400 Bariloche (Argentina)

(Received October 18, 1979)

SUMMARY

An apparatus permitting extensive plastic deformation of wires of high melting point b.c.c. metals at liquid helium temperatures is described. The recovery of the electrical resistivity of pure and oxygen-doped tantalum deformed at liquid helium temperatures was measured up to 540 K. In this temperature interval, only one major recovery stage superimposed on a continuous background recovery and located between 240 and 300 K was found. It is controlled by the long-range migration of an intrinsic point defect with a migration enthalpy of 0.70 ± 0.03 eV. The results are discussed in the context of high temperature and irradiation data, and it is concluded that the defect migrating in this "stage III" is a self-interstitial configuration.

The rate theory of the annihilation of migrating point defects with their antidefects and simultaneous reactions with unsaturable sinks (dislocations) is developed in a form that permits the quantitative analysis of the isothermal recovery curves. Its application to the present experiments gives highly consistent results and strengthens the above conclusions. The close analogy between the point defect phenomena in tantalum and α-Fe is discussed.

1. INTRODUCTION

It has been known for a long time that point defects are created during the low temperature plastic deformation of metals and that they may be investigated by studying the recovery of, say, the change $\Delta\rho$ in electrical resistivity due to cold working [1 - 5]. It is true that plastic deformation generates not only self-interstitials and vacancies but also dislocations and that the presence of high densities of dislocations will affect the point defect recovery processes. However, the investigation of point defects after cold working has two definite advantages over irradiation studies.

(i) *Irradiation* creates interstitials and vacancies in equal concentrations. As long as the principal recovery process is the mutual annihilation of interstitials and vacancies, it is difficult to obtain reliable information on the less mobile species, usually the vacancy. At temperatures at which the interstitials are highly mobile, vacancies remain only if the self-interstitials undergo "side reactions" in addition to interstitial–vacancy recombination. These side reactions of the self-interstitials (*e.g.* trapping, clustering, annihilation at jogs on dislocations etc.) lead to complications which quite often overcompensate the apparent "simplicity" of irradiation experiments. After *cold working*, the concentrations of self-interstitials and vacancies are in general different. This may facilitate the interpretation of recovery experiments.

(ii) Point defect production by plastic deformation leads in general to less-correlated point defect distributions than those resulting from irradiation. Depending somewhat on the

*Present address: École Polytechnique Fédérale de Lausanne, Laboratoire de Génie Atomique, Lausanne, Switzerland.

†Present address: Max-Planck-Institut für Metallforschung, Institut für Physik, Heisenbergstrasse 1, 7000 Stuttgart 80, F.R.G.

nature of the radiation employed, in irradiation experiments a large fraction of the point defects are produced in special configurations (*e.g.* close Frenkel pairs, vacancy clusters (depleted zones), crowdions) whose investigation may detract from the study of *isolated* interstitials or vacancies.

The preceding remarks are borne out by early studies of electrical resistance recovery after the low temperature plastic deformation of f.c.c. metals [4, 5]. Numerous experiments have shown that, after cold working, the low temperature recovery stage I is very much smaller than after irradiation [4], indicating that the defects which anneal out in stage I are associated with special configurations created preferentially by irradiation. From plastic deformation experiments, reliable information was obtained on jump frequencies and migration enthalpies of the defects migrating in recovery stages III and IV [6 - 11].

Since our knowledge of intrinsic point defects is not nearly as developed for b.c.c. metals [12 - 15] as for f.c.c. metals (see, for example, ref. 16), it appeared desirable to study the recovery of the electrical resistance of b.c.c. metals after low temperature plastic deformation. In the present work such a study was undertaken for "pure" and oxygen-doped polycrystalline tantalum deformed at liquid helium temperatures.

The investigation of point defects through recovery measurements on the b.c.c. metal tantalum after low temperature plastic deformation involves two specific problems, namely the lack of low temperature ductility of the refractory b.c.c. metals and their extreme sensitivity to interstitial impurities (see, for example, recent reviews on the deformation and work hardening of b.c.c. metals and alloys [17]). In the present study a special rolling machine was developed that permitted extensive plastic deformation at liquid helium temperatures (Section 2.2). Two different starting materials were used and subjected to purification treatments (Section 2.1).

The experimental results (Section 3) have been partly surveyed in an earlier publication [18]. The emphasis of the present paper is on the quantitative interpretation of the intrinsic "stage III" which has recently been discovered in tantalum and niobium by Faber *et al.* [19] and which occurs between 240 and 300 K in the pure tantalum used here. The experiments described in this paper confirm that this stage is associated with the long-range migration of an intrinsic point defect, presumably a self-interstitial (Sections 4.1 and 4.3).

The quantitative analysis of stage III recovery must take into account the presence of at least two different types of sinks: (1) the antidefects of the migrating defects; (2) "unsaturable" sinks, *e.g.* dislocation lines. Unfortunately, in this case not even the simplest rate equation formulation of the theory admits a closed-form solution. Therefore, some efforts have been devoted to the development of an approximate method of solution that suits the practical needs of data fitting (Section 4.2).

An interesting outcome of the present work on tantalum is the close analogy to α-Fe. This analogy is discussed in some detail in Section 4.4 and indicates that the scheme of point defect properties now established for tantalum may be of more general significance for pure b.c.c. metals.

2. EXPERIMENTAL TECHNIQUES

2.1. Sample preparation

Tantalum wires 0.25 mm in diameter were used in the deformation experiments. The starting materials were obtained from the Wah Chang Corp. or the Max-Planck-Institut für Metallforschung in Stuttgart.

The samples received from the Max-Planck-Institut had a higher initial resistance ratio ($\Gamma \equiv R_{273\,K}/R_{4.2\,K} \approx 200$) than those received from the Wah Chang Corp. and presumably contained fewer impurities initially. A purification treatment in our laboratory following Fromm and Jehn [20] and Hörz [21] (illustrated in Fig. 1) resulted in high Γ values in samples from both suppliers, those of the Stuttgart samples being somewhat higher (1700 - 2300). In order to study the influence of oxygen on the deformation and recovery processes, different amounts of oxygen were subsequently introduced by heating the wires in the temperature range 2100 - 2500 K in an oxygen atmosphere of 10^{-6} Torr.

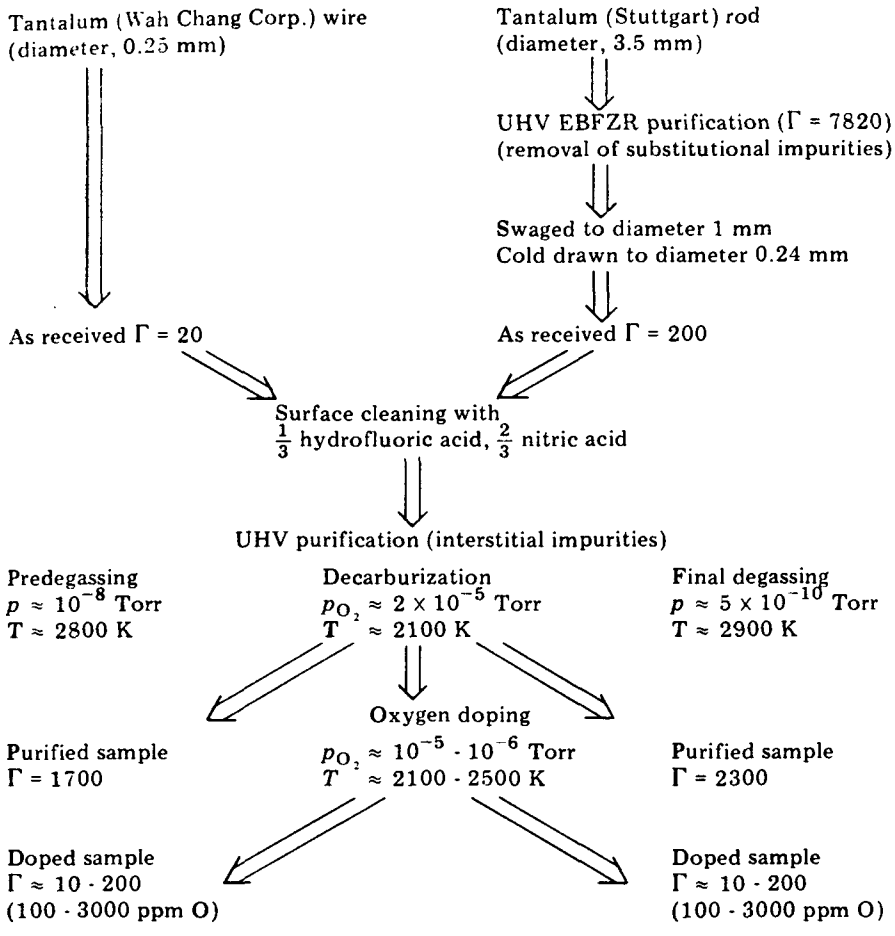

Fig. 1. Schematic representation of the purification and doping treatments: UHV, ultrahigh vacuum; EBFZR, electron beam furnace zone refinement.

2.2. Deformation and resistance measurements

The samples were deformed by rolling at 4.2 K in a small rolling mill designed in our laboratory [22]. This rolling mill consists of three main components: (i) the rolling element, a standard conical roller bearing, located inside the cryostat; (ii) the operational head of the unit, which is above and outside the cryostat and is kept at room temperature; (iii) two concentric stainless steel tubes joining (i) and (ii) and transmitting the motion necessary for deformation and release of the sample.

During the deformation the wire samples were placed in the bearing between the fixed conical race-way (the outer unit) and the rotating roller bearings (the inner unit), as shown in Fig. 2. The amount of deformation was controlled by the operational head, where the compressive force of the two units against each other was adjusted during the rotation. As a measure of the deformation we used $\epsilon = \Delta l/l_0$ where l_0 denotes the length of a wire before deformation and Δl the increase in length due to the deformation.

On completion of the deformation the samples were isolated from the rolling mill for measurement of the electrical resistance. The whole rolling mill was lifted to the upper part of the cryostat in order to reduce helium consumption, leaving the sample supported by the measuring leads. Electrical resistance measurements were made by the usual *IR* drop technique with four probes. Both ends of the sample were used as current leads. Voltage leads were attached either by spot welding the same material or by screw connectors to avoid the possibility of contamination with the lead wires passing through the bearing through slits in the race-way. Clearly it is necessary to keep the

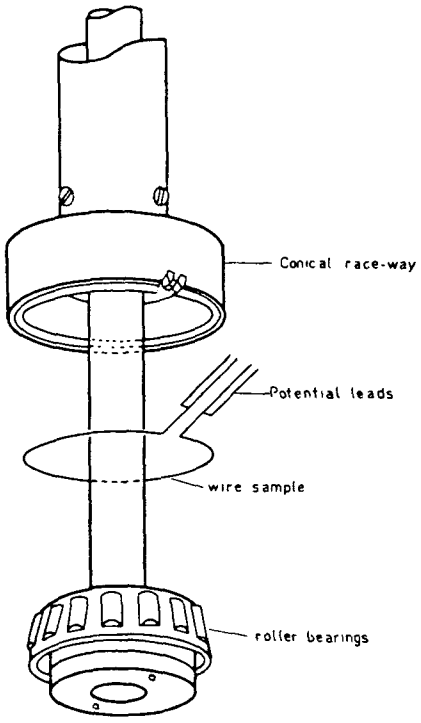

Fig. 2. The rolling element.

external stainless steel tube to which the roller race-way is connected fixed; if it turned during the deformation, the connection leads would become damaged.

The electrical resistivities at 4 K were computed from the ratios of the resistance at 4 K to that measured at 273 K with a correction to take into account that only part of the wire section between the voltage leads was deformed. For the ice point resistivity of tantalum the value $\rho_{273\,K} = 1.24$ nΩ m was used.

2.3. Annealing treatments and temperature control

The temperature gradient occurring in the cryostat was utilized for performing annealing experiments. It was found that 600 s annealing pulses in the temperature range from 4 K to near room temperature could easily be controlled to ±1 K at around 10 K and to ±0.5 K near 200 K by simply raising and lowering the sample in the cryostat. In order to obtain this good reproducibility of the temperature pulses it was necessary to avoid turbulence in the helium atmosphere above the liquid helium layer. Uniformity of the sample temperature was ensured by a double shield of polished copper foil surrounding the samples. For anneals near or above room temperature a heater mounted on the external shield was used.

During the thermal treatments the temperature was measured using a Cu–constantan thermocouple 0.1 mm in diameter covered by Teflon, one of the junctions being kept as reference at 273 K and the other in thermal contact with the sample.

3. EXPERIMENTAL RESULTS

The results of isochronal anneals between liquid helium temperature and 540 K have been presented earlier [18]. In pure tantalum (*i.e.* non-oxygen-doped samples), only one major recovery stage occurred in this temperature range, located between about 240 and 300 K (Fig. 3). As shown below, it has presumably the same origin as the stage III discovered recently by Faber *et al.* [19] after low temperature 3 MeV electron irradiation.

A remarkable feature of the present experiments is that neither the huge 165 K stage nor the recovery stages in the range from liquid helium temperature to liquid hydrogen temperature observed after the 3 MeV electron irradiation of tantalum [23, 24] can be seen. This indicates clearly that these recovery phenomena are associated with defect configurations that are characteristic of defect production by irradiation, *i.e.* they are presumably *not* due to the migration of isolated vacancies or stable self-interstitials as generated during plastic deformation.

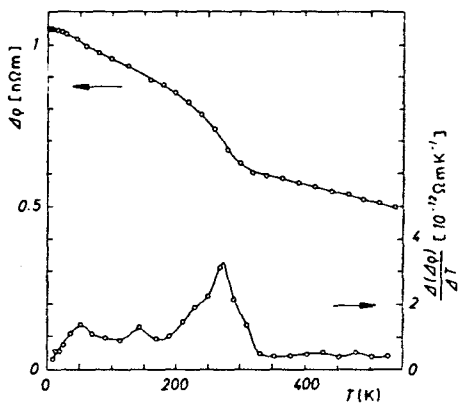

Fig. 3. Isochronal recovery of the deformation-induced electrical resistivity $\Delta\rho$ of pure tantalum (Max-Planck-Institut für Metallforschung, $\Gamma = 2330$) after low temperature deformation $\epsilon = 0.15$ for an annealing time Δt of 600 s.

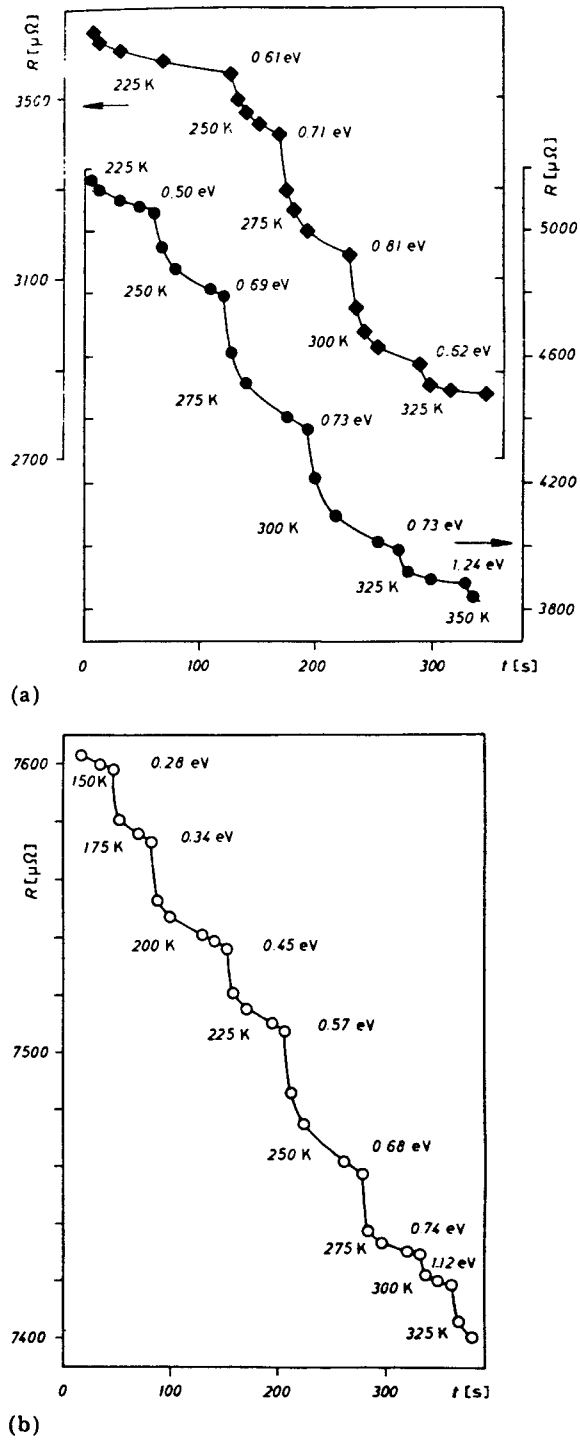

Fig. 4. Determination of activation enthalpies by the change-in-slope method (a) for pure tantalum (♦, Γ = 661; ●, Γ = 1000) and (b) for oxygen-doped tantalum (Γ = 9.1; approximately 0.27 at.% O).

Figure 4 shows the determination of effective activation enthalpies in the range 225 - 350 K for pure tantalum and in the range 150 - 325 K for oxygen-doped tantalum by means of the change-in-slope method. The precision of the individual determinations of the effective activation enthalpies is estimated to be ±6%. The mean value of the eight determinations between 250 and 325 K for pure tantalum and between 250 and 300 K for oxygen-doped tantalum is 0.71 eV. The mean values for the individual samples are not significantly different from this value. Thus it appears justified to conclude that the recovery in stage III is indeed controlled by an *intrinsic* process with a well-defined activation enthalpy.

From the information given in Fig. 4(a) we calculate the mean error of the change-in-slope measurements to be 0.02 eV. The cross-cut method based on comparison of isotherms gives an activation enthalpy of 0.70 ± 0.03 eV, so that the results of the two different techniques are in good agreement with each other.

The mean number of jumps of a point defect with migration enthalpy H_{III} = 0.70 ± 0.03 eV (and an assumed frequency factor $\nu_0 = 10^{13.5}\ s^{-1}$) during a 600 s anneal at 300 K is 10^4 - 10^5. From this order of magnitude we conclude that we are dealing with the *long-range migration* of a point defect that may be generated by plastic deformation and that possesses a well-defined migration enthalpy.

The following comparison of recovery temperatures observed after plastic deformation or electron irradiation indicates that the defects just described are identical with those responsible for stage III after electron irradiation. In Fig. 5 we plotted on a logarithmic scale the irradiation- or deformation-induced resistivity remaining at the beginning of stage III (full symbols) or recovering in stage III (open symbols) against the reciprocal temperature of the centre of the stage. It is evident that the data obtained after deformation (squares) constitute the "continuation" of the irradiation data (circles and triangles) towards higher resistivities and lower temperatures. The broken line indicates the slope that would be expected for a *second-order* reaction with an activation enthalpy of 0.71 eV. We shall see in Section 4 that at least in deformed samples the reaction kinetics are more complicated than second order.

Also included in Fig. 5 are data points corresponding to a recovery stage at about

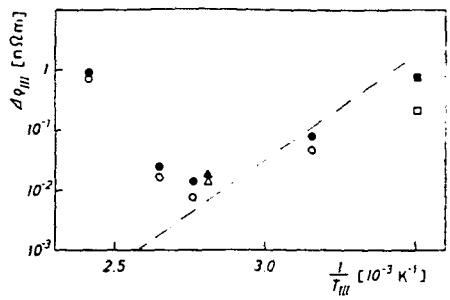

Fig. 5. Logarithm of stage III resistivity recovery in pure tantalum as a function of the reciprocal of temperature T_{III} in isochronal recovery experiments (for a holding time Δt of 600 s): open symbols, residual resistivity $\Delta\rho_{III}$ annealing out in stage III; full symbols, excess residual resistivity $\Delta\rho_{III+rest}$ at the beginning of stage III; ●, ○, 3 MeV electron irradiation at 4.5 K [23]; ▲, △, 3 MeV electron irradiation at 34 K [23]; ■, □, plastic deformation at 4.2 K (Stuttgart material, ϵ = 15%).

415 K observed by Schweikhardt [23] after a high dose electron irradiation. This recovery process is clearly distinct from stage III and must be governed by a different mechanism. A proposal for the nature of the 415 K recovery will be made in Section 4.1.

Figures 6 and 7 show isothermal recovery curves of the residual electrical resistance R in the temperature range of stage III. The full curves represent the fits to be described in Section 4.2, the value $R(\infty)$ marking the end of stage III according to these fits. In most cases the short-time experimental data show well-defined deviations from the fits. The short-time measurements may be described by a $t^{1/2}$ law. The resistance extrapolated to $t = 0$ according to this law is indicated by $R(0)$. The total resistivity $\Delta\rho_{III}$ recovering in stage III was calculated from the difference $R(0) - R(\infty)$ and is included in Table 1.

4. DISCUSSION

4.1. General observations

The most significant experimental results discussed in this paper are the following.

(i) The recovery stage III in tantalum, first recognized after low temperature electron irradiation [19], is also observed after low temperature plastic deformation.

(ii) No other well-developed recovery stage was found in plastically deformed pure tantalum between 4.2 and 540 K.

(iii) Stage III recovery in tantalum is governed by the long-range migration of an intrinsic defect with a migration enthalpy $H_{III} = 0.71 \pm 0.03$ eV.

The shape of the electron irradiation damage curves at 4.2 K as observed by Schweikhardt [23] suggests that an intrinsic defect, presumably an intersitital configuration, is capable of migrating freely below 4.2 K. The low temperature recovery stages observed after electron irradiation at 4.2 K are presumably associated with defect configurations formed during the migration of these defects, *e.g.* those at 14 K with the annihilation of a very unstable close Frenkel pair. The absence of these low temperature recovery stages after plastic deformation is most easily accounted for by the hypothesis that the ultramobile low temperature defects are *not* formed (at least not to a detectable extent) during cold working. This suggests (1) that these defects are metastable, (2) that a second stable self-interstitial configuration exists and (3) that the "low temperature" defects are generated by a process that is characteristic of radiation damage, *e.g.* a process involving replacement collision chains.

The preceding hypotheses are supported by the observation that the shape of the damage curves below about 120 K is as if two self-interstitial configurations are produced, a mobile configuration and an immobile configuration [23, 25]. An example that satisfies all the known requirements for the ultramobile low temperature defect in tantalum is provided by the crowdion-type interstitial configuration which may indeed result from replacement collision chains propagating approximately in the close-packed direction.

Among the recovery stages so far observed in irradiated or plastically deformed tantalum, only stage III has the characteristic features corresponding to free migration of an intrinsic point defect. From the above discussion, however, we expect to find at least two such stages above liquid helium temperature, one associated with the migration of the stable interstitial configuration and the other associated with vacancy migration. It is clear that resistivity measurements after irradiation or cold working alone do not allow us to decide whether the free-migration stage actually observed is due to interstitial or vacancy migration. The analysis of the present

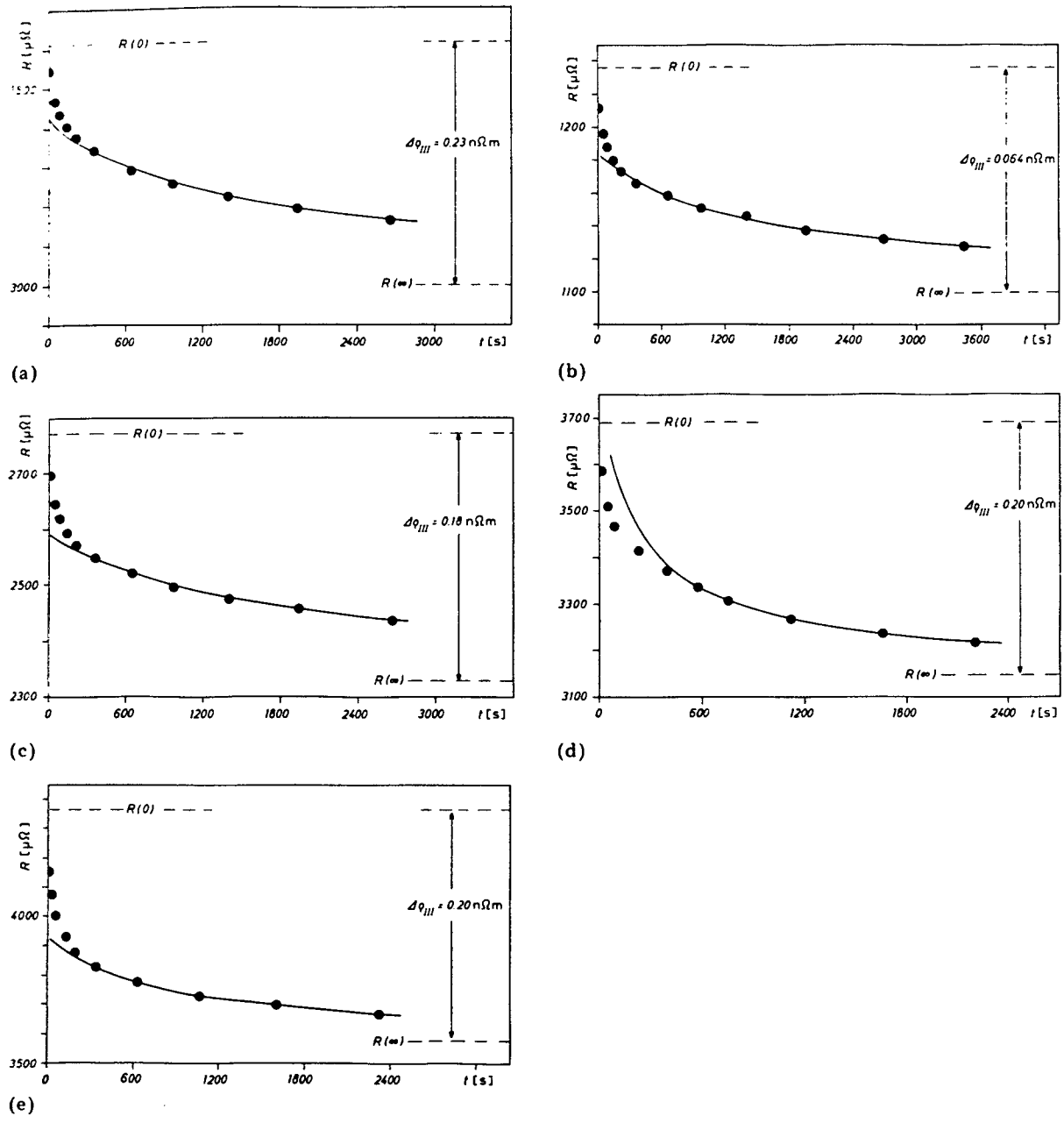

Fig. 6. Isothermal recovery at different temperatures T of the electrical resistance of pure tantalum (for various residual resistance ratios Γ) deformed near 4.2 K by different strains ϵ: (a) Γ = 1170, ϵ = 25%, T = 265 K; (b) Γ = 1220, ϵ = 3.9%, T = 275 K; (c) Γ = 989, ϵ = 15%, T = 275 K; (d) Γ = 973, ϵ = 32%, T = 275 K; (e) Γ = 1470, ϵ = 17%, T = 290 K.

stage III data to be developed in Section 4.2 in fact does not distinguish between interstitials and vacancies, although for reasons to be given we based its explicit formulation on the assumption that in stage III interstitials are mobile and vacancies are immobile.

Evidence for the mobility of the vacancies in tantalum is provided by high temperature positron annihilation experiments (which give information on the monovacancy formation enthalpy) and by self-diffusion measurements (from which the sum of vacancy formation and migration enthalpies may be obtained). Maier *et al.* [26] have concluded that their positron annihilation experiments on tantalum are *not* compatible with vacancy

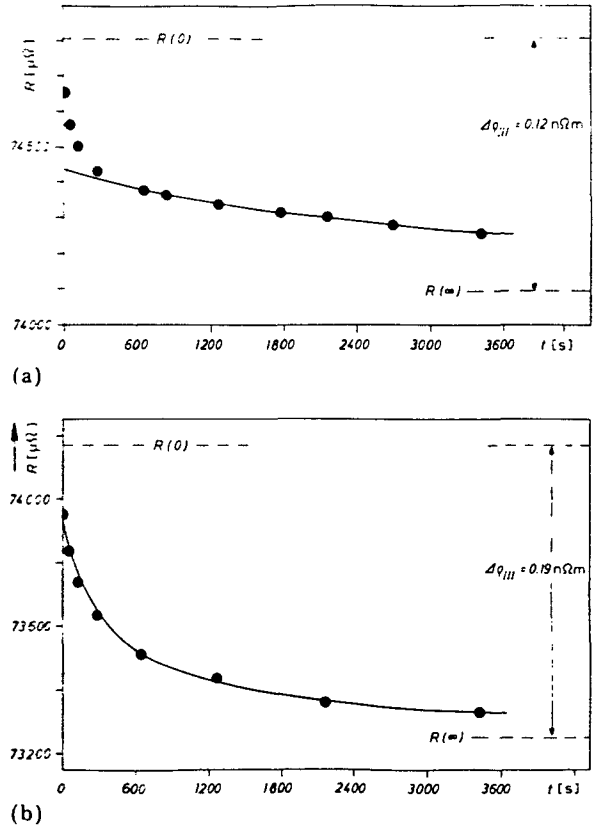

Fig. 7. Isothermal recovery at two annealing temperatures for oxygen-doped tantalum (2700 at.ppm O) deformed near 4.2 K: (a) $\Gamma = 10$, $\epsilon = 17\%$, $T = 210$ K; (b) $\Gamma = 10$, $\epsilon = 17\%$, $T = 250$ K. The formal fit of eqn. (12) shown in Fig. 7(a) corresponds to $\tau = 1.4 \times 10^5$ s, $\gamma = 19.5$ and $x_0 = 6.1$.

migration in stage III and that vacancy migration is in fact expected above the temperature range covered by the *present* measurements. This conclusion is in good agreement with the absence of a second free-migration stage in the present recovery experiments and with a recent analysis of the behaviour of foreign interstitial atoms in the group V transition metals [27]. Recent more extensive positron annihilation experiments, which also include other group V transition metals (niobium, vanadium) as well as molybdenum and tungsten, have strengthened the above conclusions [28].

On the basis of the evidence just described we attribute the stage III recovery of tantalum to the migration of self-interstitials with a migration enthalpy $H_I^M = 0.71 \pm 0.03$ eV. In the present experiments the principal sinks for these interstitials are thought to be (immobile) vacancies and dislocation lines. In addition, impurities (in particular foreign interstitial atoms) may act as traps for the migrating self-interstitials. A rate equation treatment of this simple model is given in Section 4.2. We shall see that it is indeed capable of describing the present kinetic data adequately with the exception of short annealing times where we cannot expect the rate equation approach to be valid. Nevertheless, because stage III is suppressed after very high irradiation doses (the radiation-induced resistivity change $\Delta\rho_0$ after 4.5 K irradiation is equal to 5 nΩ m) and because a new recovery stage appears at higher temperatures (about 415 K) [23], the preceding picture may be oversimplified. The observed phenomena are very similar to those found in electron-irradiated platinum [29]. For platinum, sufficient experimental results are available to permit a reliable interpretation [30, 31]. Prolonged irradiation results in the spatial separation of interstitials and vacancies by radiation-induced diffusion and the Lück–Sizmann effect [32 - 34]. In platinum (and presumably also in tantalum) the interstitial–interstitial interaction is relatively strong; after high dose irradiation this leads to interstitial clustering at the expense of interstitial–vacancy recombination. In tantalum irradiated at liquid helium temperature the Lück–Sizmann effect is enhanced since (in contrast with the corresponding platinum experiments) the metastable interstitials are mobile at the irradiation temperature and may be trapped by stable interstitials or their clusters.

Small self-interstitial clusters may break up by first-order reactions at higher temperatures. From the break-up temperature of 415 K we estimate a dissociation energy of 1.3 - 1.4 eV for tantalum and hence an effective interstitial binding energy of 0.6 - 0.7 eV. These values are essentially the same as those deduced for platinum. The hypothesis of extensive interstitial clustering in high dose irradiations ($\Delta\rho_0 \approx 5$ nΩ m) of tantalum also accounts for the observation of a high concentration of extended defects in transmission electron microscopy [23], whereas after irradiation up to $\Delta\rho_0 \approx 1$ nΩ m no visible damage could be detected.

Finally in this section we discuss the influence of oxygen doping on the recovery

TABLE 1

Specimen characteristics and the results of the analysis of the isothermal annealing data in terms of the kinetic theory of Section 4.2

Parameter	*Annealing curve for pure samples*					*Annealing curve for doped sample, ≈ 2700 ppm O, Fig. 7(b)*
	Fig. 6(a)	*Fig. 6(b)*	*Fig. 6(c)*	*Fig. 6(d)*	*Fig. 6(e)*	
Residual resistance ratio Γ	1170	1220	989	973	1470	10
Plastic deformation ϵ (%)	25	3.9	15	32	17	17
Resistivity increase $\Delta\rho_0$ due to cold working (nΩ m)	1.59	0.54	1.01	1.51	1.41	2.10
Annealing temperature T (K)	265	275	275	275	290	250
Resistivity recovery $\Delta\rho_{III}$ in stage III (nΩ m)	0.23	0.06	0.18	0.20	0.20	0.19
Analysis of kinetics						
τ ($\times 10^3$ s)	62.4	19.3	29.8	33.6	9.1	73.0
γ	49	6.6	1.8	13	1.9	125
x_0	7.1	4.1	3.4	7.0	3.2	9.5
Physical parameters deduced						
$C_V(\infty)/C_V(0)$	8×10^{-4}	2×10^{-2}	3×10^{-2}	9×10^{-4}	4×10^{-2}	(7×10^{-5})
$C_I(0)/C_V(0)$	1.3	1.4	1.2	1.1	1.2	(1.1)
$C_V(0)$	1.2×10^{-5}	3×10^{-6}	1.0×10^{-5}	1.1×10^{-5}	1.1×10^{-5}	(1.1×10^{-5})
$C_V(\infty)$	1×10^{-8}	5×10^{-8}	3×10^{-7}	1×10^{-8}	4.4×10^{-7}	(8×10^{-10})
D_I°/a_0^2 ($\times 10^{12}$ s^{-1})	21	28	8	43	4	(600)
Λ_{eff} (m^{-2})	2.2×10^{14}	1.5×10^{14}	2.6×10^{14}	0.6×10^{14}	3.8×10^{14}	(0.5×10^{14})

The physical parameters pertaining to the oxygen-doped sample are in parentheses in order to indicate that the assumptions made in their derivation are likely to be inadmissible and that the parameters should only be regarded as a formal description of the experimental results.

after low temperature cold working. Doping with 0.27 at.% O has two effects.

(i) It shifts stage III to lower temperatures by about 24 K [18] without changing its activation enthalpy significantly. This corresponds to a reduction in the number of jumps by a factor of 20 and can be explained by the trapping of migrating self-interstitials by interstitially dissolved oxygen atoms.

(ii) An additional recovery is observed somewhat below stage III [18]. As may be seen from Fig. 4(b), here the effective activation enthalpies are only about one-half of the stage III activation enthalpies. It is obvious that these enthalpies cannot correspond to the migration enthalpy of well-defined defects. Rather, the observed recovery is presumably due to rearrangements within complexes built up from intrinsic defects and oxygen atoms that had been preferentially formed during the plastic deformation of the doped material.

4.2. Quantitative analysis of stage III annealing kinetics: theory

On the basis of the evidence discussed in Section 4.1, we assume that the basic features of stage III recovery is the migration of simple point defects in the presence of an essentially random distribution of their antidefects. The annihilation of a defect–antidefect pair (a Frenkel pair) results in a resistivity decrease ρ_{FP} (per unit concentration). Alternatively, in the strongly deformed samples used in the present experiments the migrating defects may reach dislocations and disappear at jogs or become immobilized. Another possibility is that the migrating defects are trapped at impurities or pre-existing point defect clusters.

The simplest possible description of the preceding reactions is in terms of the rate equations

$$\frac{dC_I}{dt} = -\alpha C_I C_V - \beta C_I \tag{1a}$$

$$\frac{dC_V}{dt} = -\alpha C_I C_V \tag{1b}$$

where C_I denotes the atomic concentration of the mobile defects and C_V the atomic concentration of their (immobile) antidefects. (The present notation is chosen in accordance with the view that the migrating defects are self-interstitials and their immobile antidefects are vacancies, but an interchange of vacancies and interstitials would clearly leave the time dependence of ρ (eqn. (3)) unchanged. As shown in Appendix A, another change in the dependent variables transforms eqns. (1) into the basic equations of epidemiology.) The coefficients α and β are both proportional to the diffusion coefficient D_I of the mobile species. According to Waite's theory [26] the first of these may be written as

$$\alpha = \frac{4\pi r_{VI} D_I}{V_A} \tag{2}$$

where r_{VI} denotes the radius of recombination of interstitials and vacancies and V_A the atomic volume. The β term in eqn. (1a) takes into account all the other processes discussed above (the disappearance of point defects at dislocations and trapping); it is assumed that β is independent of C_I and C_V, *i.e.* that we are dealing with *unsaturable* sinks or traps.

If we assume the contribution of the unsaturable sinks to be independent of the number of point defects that they have absorbed, the electrical resistivity is given by

$$\rho = \rho_I C_I + \rho_V \{C_V - C_V(\infty)\} + \rho(\infty) \tag{3}$$

where ρ_I and ρ_V are the electrical resistivities per unit concentration of self-interstitials or vacancies ($\rho_I + \rho_V = \rho_{FP}$). In eqn. (3) $\rho(\infty)$ denotes the electrical resistivity and $C_V(\infty)$ the vacancy concentration remaining after completion of the recovery.

Equations (1) have been discussed repeatedly in the literature. Although they form the simplest possible description of the processes under discussion, they cannot be explicitly solved in closed form. In view of the frequent occurrence of eqns. (1) in annealing problems, it is desirable to develop numerical methods of solution that permit a straightforward comparison with experimental data.

Elimination of the time t gives us the first-order differential equation

$$\frac{dC_I}{dC_V} = 1 + \frac{\beta}{\alpha}\frac{1}{C_V} \tag{4}$$

with the integral

$$C_I = C_V - C_V(\infty) + \frac{\beta}{\alpha}\ln\left\{\frac{C_V}{C_V(\infty)}\right\} \tag{5}$$

As the constant of integration in eqn. (5) we chose the vacancy concentration $C_V(\infty)$ at the end of the reaction, *i.e.* after an infinitely long time. The end of the reaction is marked by the disappearance of all mobile defects (*i.e.* $C_I = 0$). Even if the initial concentration $C_I(0)$ of the mobile defects is larger than the initial concentration $C_V(0)$ of their anti-defects, at the end of the reaction a positive concentration $C_V(\infty)$ of immobile defects will always remain, provided that β is positive. ($\beta = 0$ would correspond to the absence of non-saturable traps or sinks and leads to the well-known closed-form solutions of eqns. (1), so that we may indeed confine ourselves to $\beta > 0$.) The reason for this is that, as C_V becomes smaller and smaller because of the recombination process, the non-saturable sinks and/or traps will eventually dominate the reaction and a finite concentration $C_V(\infty)$ will remain.

For the further treatment of eqns. (1) it is convenient to characterize the reaction by the dimensionless variable

$$x(t) \equiv \ln\left\{\frac{C_V(t)}{C_V(\infty)}\right\} \tag{6}$$

It decreases from

$$x_0 = \ln\left\{\frac{C_V(0)}{C_V(\infty)}\right\} \tag{6a}$$

at the beginning of the reaction to zero at its end. Insertion of eqns. (5) and (6) into eqn. (1a) gives us the following first-order differential equation for $x(t)$:

$$\frac{dx}{dt} = -\alpha C_V(\infty)\{\exp(x) - 1 + \gamma x\} \tag{7}$$

with the dimensionless parameter

$$\gamma \equiv \beta/\alpha C_V(\infty) \tag{7a}$$

Integration of eqn. (7) results in

$$\alpha C_V(\infty)t = \int_{x'=x(t)}^{x_0} \frac{dx'}{\exp(x') - 1 + \gamma x'} \tag{8}$$

The parameter x_0 characterizes not only the initial concentration $C_V(0)$ through eqn. (6a) but also, together with γ, the initial ratio of the defect concentrations according to

$$\frac{C_I(0)}{C_V(0)} = 1 + (\gamma x_0 - 1)\exp(-x_0) \tag{9}$$

We see that the present theory contains three adjustable parameters, namely the dimensionless parameters γ and x_0 and the quantity $\alpha C_V(\infty)$ which has the dimension of a reciprocal time. For a given annealing run the quantities γ and x_0 have to be found by fitting the *shapes* of the isothermal annealing curves to the theoretical expression (8), whereas $\alpha C_V(\infty)$ must be deduced from a comparison of the *physical time scale* with that resulting from the fit. In practice, the electrical resistivity $\rho(\infty)$ at the end of the reaction must be included in the fitting procedure as a fourth parameter since, because of possible small contributions of recovery processes other than those included in eqns. (1), the final resistivity $\rho(\infty)$ cannot usually be read off from the experimental data directly with the required accuracy.

Equation (8) cannot be integrated in closed form. We shall develop an approximate procedure for determining $x(t)$ that allows three of the four adjustable parameters (namely γ, $\alpha C_V(\infty)$ and $\rho(\infty)$) to be found, at least approximately, from fitting simple *analytical* expressions to the experimental data. The fourth parameter x_0 appears only at a later stage of the approximation procedure which at the same time allows us to test, and if necessary to correct, the earlier steps.

The integral (8) was written in a form that is convenient for an approximation procedure starting at long times and working towards shorter times. This is a reasonable procedure from a physical point of view, since at short times correlated recovery processes may occur that are not adequately accounted for by rate equations but require a description in terms of diffusion equations (see below).

For $|x| \ll 1$ we may write

$$\exp(x) - 1 + \gamma x = x\left(1 + \gamma + \frac{x}{2}\right) + O(x^3) \tag{10}$$

Addition and subtraction of the reciprocal of the right-hand side of eqn. (10) gives the identity

$$\frac{1}{\exp(x)-1+\gamma x} \equiv \frac{x^2-2\{\exp(x)-1-x\}}{2x\{\exp(x)-1+\gamma x\}(1+\gamma+x/2)} + \frac{1}{1+\gamma}\left\{\frac{1}{x}-\frac{1}{x+2(\gamma+1)}\right\} \tag{11}$$

By inserting eqn. (11) into eqn. (8) and integrating we obtain the solution of eqns. (1) in the form

$$\ln\left\{\frac{x+2(1+\gamma)}{x}\right\} + f(x;\gamma) = \alpha C_V(\infty)(1+\gamma)t + \left[\ln\left\{\frac{x_0+2(1+\gamma)}{x_0}\right\} + f(x_0;\gamma)\right] \tag{12}$$

with

$$f(x;\gamma) \equiv (1+\gamma)\int_0^x \frac{2\{\exp(x)-1-x\}-x^2}{2x\{\exp(x)-1+\gamma x\}(1+\gamma+x/2)}\,dx \tag{13}$$

Equation (12) has the interesting feature that in the relationship $x = x(t)$ the adjustable parameter x_0 appears in a term that affects only the origin of the time scale, *i.e.* a term that is of minor importance in the fitting of eqn. (12) to the isotherms at long times. Furthermore, at long times, *i.e.* for $|x| \ll 1$, we have

$$f(x;\gamma) = \frac{x^2}{12(1+\gamma)} + O(x^3) \tag{14}$$

This means that for sufficiently long times we may replace eqn. (12) by

$$\ln\left\{1+\frac{2(1+\gamma)}{x}\right\} = \frac{t+t_0}{\tau} \tag{15}$$

with

$$\tau^{-1} \equiv \alpha C_V(\infty)(1+\gamma) = \alpha C_V(\infty) + \beta \tag{16}$$

and

$$t_0 \equiv \tau\left[\ln\left\{1+\frac{2(1+\gamma)}{x_0}\right\} + f(x_0;\gamma)\right] \tag{17}$$

Equation (15) may be rewritten as

$$x(t) = \frac{2(1+\gamma)}{\exp\{(t+t_0)/\tau\}-1} \tag{18}$$

The form of eqn. (18) is well known from the theory of bimolecular reactions with unequal initial concentrations of the reaction partners, although with the difference that, in eqn. (18), x is not proportional to but logarithmically dependent on the concentration (see eqn. (6)). At very long times eqn. (18) reduces to first-order reaction kinetics with decay time τ given by eqn. (16). If the experimental data extend to sufficiently long times it is possible to deduce τ directly; otherwise a fit of eqn. (18) to the *shape* of the recovery curve at long times must be attempted. This results in numerical values of τ, γ and $\rho(\infty)$. Using the γ value obtained in this way the function $f(x;\gamma)$ may be calculated numerically. The parameter x_0 (which according to eqn. (17) also determines t_0) must be determined by fitting eqn. (12) to the experimental data. If the fit is not satisfactory, we can change the γ value somewhat and can try to find a consistent pair of γ and x_0 values. According to eqn. (9) this pair gives us the ratio $C_I(0)/C_V(0)$ of the concentration of the self-interstitials to the concentration of the vacancies at the beginning of the recovery.

The final set of parameters obtained will be a compromise between as good a fit as possible at long times, where the rate theory is expected to describe the experiments well, and the tendency to apply the theory over as wide a range of annealing times as possible. The present rate theory treatment of the stage III problem is known to fail at short times and has to be replaced by a diffusion theory. On general grounds the diffusion theory predicts a $t^{1/2}$ recovery law at short times. As already mentioned in Section 3, the short-time measurements are indeed well described by a $t^{1/2}$ law. In this respect they are similar to the data of Cuddy [35] on the stage III resistivity recovery of pure α-Fe [36].

4.3. Quantitative analysis of stage III annealing kinetics: results

The full curves in Figs. 6 and 7 give the fit of the theory of Section 4.2 to the resistance measurements. Table 1 lists for a number of runs the kinetic parameters resulting from these fits and the physical quantities deduced

from them. In these fits ρ_I/ρ_V was treated as a fixed parameter. The quality and the results of the fits are not sensitive to the precise choice of ρ_I/ρ_V. The numerical values given for pure samples correspond to $\rho_I/\rho_V = 1.09$.

We see that in all runs the concentration $C_I(0)$ of the self-interstitials at the beginning of stage III was larger than the corresponding vacancy concentration $C_V(0)$, although in no case by more than 50%. The vacancy concentration $C_V(\infty)$ at the end of stage III is small compared with $C_V(0)$. This shows that the majority of the self-interstitials disappear by recombination with vacancies, although because $C_I(0) > C_V(0)$ a substantial fraction of them must have gone to dislocation sinks.

In view of the results of the preceding paragraph we shall not incorporate a large error if we assume that $\rho_I = \rho_V = \rho_{FP}/2$ and calculate the vacancy concentration at the beginning of stage III by means of the approximate formula

$$C_V(0) \approx \frac{2}{1 + C_I(0)/C_V(0)} \frac{\Delta\rho_{III}}{\Delta\rho_{FP}} \tag{19}$$

Together with the resistivity per unit concentration of Frenkel pairs,

$$\rho_{FP} = 17\ \mu\Omega\ \text{m} \tag{20}$$

deduced from radiation damage experiments [37], this gives us the vacancy concentrations at the beginning and the end of stage III listed in Table 1. The values derived in this way for the pure samples appear to be of a reasonable order of magnitude.

From eqns. (2) and (16) we obtain the relationship

$$D_I = \frac{V_A}{4\pi r_{VI} C_V(\infty)(1 + \gamma)\tau} \tag{21}$$

between the self-interstitial diffusion coefficient

$$D_I = D_I^\circ \exp\left(-\frac{H_I^M}{kT}\right) \tag{22}$$

and the characteristic recovery time τ. Together with $H_I^M = 0.71$ eV and the estimate $r_{VI}/a_0 = 2$ (where the lattice parameter a_0 of tantalum is 3.3×10^{-10} m; $V_A = a_0^3/2$), the insertion of the numerical values of Table 1 into eqn. (21) gives us the pre-exponential factor D_I°/a_0^2 of Table 1. Within the uncertainties expected from the accumulation of errors during the analysis, the results of the various runs on pure samples are in satisfactory agreement with each other. The average of the various runs is

$$D_I^\circ/a_0^2 = 2 \times 10^{13}\ \text{s}^{-1} \tag{23}$$

The order of magnitude of eqn. (23) is very reasonable; this can be seen as follows. We may write

$$D_I^\circ = g_I a_0^2 \nu_0 \exp\left(\frac{S_I^M}{k}\right) \tag{24}$$

where g_I denotes a geometrical factor depending on the (unknown) configuration and migration mechanism of the self-interstitials, ν_0 an atomic attempt frequency and S_I^M the migration enthalpy of the self-interstitials. g lies presumably between one-half and unity. We thus obtain the result that for self-interstitials in tantalum

$$\nu_0 \exp\left(\frac{S_I^M}{k}\right) \approx (2 - 4) \times 10^{13}\ \text{s}^{-1} \tag{25}$$

which is slightly larger than the attempt frequency ν_0 that may be estimated from the atomic mass and the lattice parameter of tantalum, in agreement with the general experience that in metals interstitial migration entropies are positive.

In spite of the fact that Fig. 7(b) shows an excellent fit of the theory to the experimental data (for $\rho_I/\rho_V = 0.7$), the large value of D_I°/a_0^2 found for the oxygen-doped sample annealed at 250 K indicates that the theory does not adequately account for these data. The reason is that in this run the oxygen atoms are the main traps for migrating self-interstitials and that they can be described neither as unsaturable traps nor as recombination centres (*i.e.* saturable traps). Nevertheless the experiments are in good accord with the results so far deduced; this can be seen as follows.

Let C_O denote the atomic concentration of oxygen traps and r_{OI} their capture radius for self-interstitials. Since C_O is presumably larger than $C_I(0)$, we expect to find approximate first-order kinetics with a time constant

$$\tau = \frac{V_A}{4\pi r_{OI} D_I C_O} \tag{26}$$

The exceptionally large γ value in Table 1 indicates that the observed kinetics are close to first order. From Fig. 7(b) we estimate that $\tau = 10^3$ s; hence, with $r_{OI} = a_0$ and D_I as given above, $C_O = 4 \times 10^{-4}$. Thus the oxygen concentration in the sample is sufficient to account for the observed trap concentration even if some of the oxygen atoms have clustered.

In the cases in which the unsaturable sinks are mainly dislocation lines (and not foreign atoms) we may write

$$\beta = D_I \Lambda_{eff} \tag{27}$$

where Λ_{eff} is an "effective" dislocation density. The effective character of Λ_{eff} stems from the fact that it includes the capture or trapping radius of the dislocations for the defects migrating in stage III, which depends on the dislocation character.

The equation

$$\Lambda_{eff} = \frac{4\pi r_{VI} \gamma C_V(\infty)}{V_A} \tag{28}$$

which follows from eqns. (2), (7a) and (27) permits us to obtain the order of magnitude of the effective dislocation density in the deformed samples. Using the same estimate as above ($r_{VI}/a_0 = 2$), the Λ_{eff} values given in Table 1 are obtained.

The general order of magnitude ($\Lambda_{eff} = 2 \times 10^{14}$ m^{-2}) is as expected for plastic deformation by the amounts used here. There is no clear-cut correlation between the deformation ϵ and the effective dislocation density. This may simply be because the dislocation density of deformed metals is more directly related to the flow stress (unknown in the present case) than to the degree of deformation, particularly in complex deformation modes such as are employed in this work.

The deformation-induced resistivity remaining after stage III annealing is typically of the order of magnitude 0.5 nΩ m. If in view of the small residual vacancy concentration $C_V(\infty)$ it is mainly attributed to dislocations and if for the purpose of an order-of-magnitude estimate we identify Λ_{eff} with the dislocation density, we find the resistivity per unit dislocation length per unit volume to be approximately 2.5×10^{-24} Ω m^3. This is a reasonable order of magnitude compatible with the data on other metals (see, for example, the results on edge dislocations in the noble metals [38]).

Summarizing the conclusions of this section, we may say that the quantitative analysis of the experimental data of the present paper based on the theory of Section 4.2 leads to a high degree of internal consistency and that the results obtained are also consistent with established results on other metals. We take this as an indication of the reliability of the proposed approach and of the potential of cold-working experiments for obtaining reliable data on the migration of intrinsic point defects in metals.

4.4. Relationship to recovery experiments on deformed α-Fe

Cuddy [35] deformed high purity iron (of resistance ratio $\Gamma = 2800$) by different amounts at 77 K and investigated the recovery of the electrical resistivity up to 520 K. The results bear several similarities to the present experiments. Since they may help us to gain a more general perspective of the recovery processes in pure b.c.c. metals, we shall discuss them in this section.

As for tantalum, only one major recovery stage centred at about 210 K for 600 s isochrones was observed. The differences in the temperatures of deformation and hence in the lowest annealing temperatures are thought to be of minor importance, since in contrast with tantalum from radiation damage experiments on α-Fe there is no evidence for long-range free migration of an intrinsic point defect migrating below liquid nitrogen temperature [13].

The recovery stage at 210 K in α-Fe is in many respects similar to the 270 K stage in tantalum investigated in the work reported in this paper, so that it should also be labelled as stage III. From the results of Cuddy [35] it follows that the enthalpy H_{III} of migration in this stage is 0.55 ± 0.02 eV. Within experimental error its ratio to the temperature T_{III} of the stage centre is the same ($H_{III}/kT_{III} = 30$) as for the tantalum recovery stage. This supports the idea that in both metals the recovery is governed by the same processes. It has already been remarked (Section 4.2) that the initial recovery kinetics are the same in α-Fe and tantalum. If the resistivity $\Delta\rho(\infty)$ at the end

of stage III recovery is treated as a quantity to be found from the analysis (as it should be), the kinetics of Section 4.2 lead to good fits for α-Fe also. Cuddy fitted his results (with a different choice of $\Delta\rho(\infty)$) to a modification of the so-called Bullough–Newman kinetics [39]. However, the physical meaning of the required modification remains unclear, and the enthalpy of migration obtained from the fit (0.50 eV) is not in good agreement with the values obtained from the so-called cross-cut method, in which fewer assumptions are made. We therefore believe that the interpretation of the iron results in terms of the theory of Section 4.2 is more appropriate.

On the grounds that in radiation damage experiments the free migration of intrinsic point defects, presumably self-interstitials, has been seen at about 110 K, Cuddy [35] assumed that the defects migrating in the 210 K stage in α-Fe are monovacancies. However, in the meantime it has been demonstrated [40 - 43] that in α-Fe monovacancies migrate at much higher temperatures and that they are definitely immobile during the 210 K anneals.

However, in Cuddy's experiments the 110 K recovery is absent or at least very much smaller than the 210 K recovery. Kaneko *et al.* [44] have investigated the temperature regime in question (stage I) in more detail on iron wires (Γ = 400 without correction for size effect and ferromagnetism) deformed at 50 or 70 K. Between 80 and 170 K they observed several small recovery stages of the electrical resistance but no clear-cut analogue to the large free-migration stage observed after low temperature irradiation by several experimental techniques (*e.g.* electrical resistivity measurements [45, 46], magnetic after-effect [47]). The situation thus appears very similar to that in f.c.c. metals, as discussed in Section 1. It suggests that the defects migrating in stage I in α-Fe (presumably self-interstitials) possess configurations that are preferentially produced by irradiation and *not* by cold working, whereas stage III is controlled by the migration of a more stable self-interstitial configuration (with a migration enthalpy H_I^M of 0.55 ± 0.02 eV). This is in agreement with the viewpoints of Nihoul [13] and Schaefer *et al.* [42], as well as with the conclusions of Decker *et al.* [48] drawn from an extensive set of experiments on the stage III defect in α-Fe. The application of the theory of Section 4.2 indicates that, as in pure tantalum, in Cuddy's experiments the principal sinks for these self-interstitials are vacancies and dislocations.

Apart from the differences in the low temperature recovery after irradiation the analogies in the point defect phenomena in the group V transition metals including tantalum and in α-Fe are indeed very close. Elsewhere it has been shown [27] that these analogies extend to the interaction between foreign interstitial atoms and vacancies in the temperature regime between stages III and IV (the monovacancy migration stage). They also include the correlation [49] of stage III migration enthalpies in b.c.c. metals by means of Flynn's theory [50] if we take into account that this theory does not discriminate between interstitial and vacancy migration and that therefore it may be applied to self-interstitial migration in stage III.

ACKNOWLEDGMENTS

The authors are indebted to Professor G. Schöck, now at the University of Vienna, who initiated the present experiments, to Lic. M. Balanzat, now at the Centre d'Études Nucléaires de Grenoble, for his collaboration in the analysis of the iron experiments and numerous discussions and to Lic. G. Sánchez Sarmiento, Bariloche, for developing the computer program used in the fitting of the kinetic theory of Section 4.2 to the experimental data. They also acknowledge gratefully critical discussions with Professor W. Frank and Professor H. Schultz as well as the support by the Gesellschaft für Kernforschung, Karlsruhe, through the programme of the German–Argentine cooperation in the peaceful application of nuclear energy.

REFERENCES

1 F. Seitz, *Adv. Phys.*, *1* (1953) 43.
2 A. Seeger, Theorie der Gitterfehlstellen, *Handb. Phys.*, *3* (1) (1955) 383.
3 H. G. van Bueren, *Imperfections in Crystals*, North-Holland, Amsterdam, 1960.
4 M. Swanson, *Phys. Status Solidi A*, *3* (1969) 287, 551.

5 A. van den Beukel, in A. Seeger, D. Schumacher, W. Schilling and J. Diehl (eds.), *Vacancies and Interstitials in Metals*, North-Holland, Amsterdam, 1970, p. 427.
6 R. R. Eggleston, *J. Appl. Phys., 23* (1952) 1400.
7 D. Schumacher, W. Schüle and A. Seeger, *Z. Naturforsch., 17a* (1962) 228.
8 F. Ramsteiner, W. Schüle and A. Seeger, *Phys. Status Solidi, 2* (1962) 1005.
9 W. Schüle, A. Seeger, D. Schumacher and K. King, *Phys. Status Solidi, 2* (1962) 1199.
10 P. Simson and R. Sizmann, *Z. Naturforsch., 17a* (1962) 596.
11 F. Ramsteiner, W. Schüle and A. Seeger, *Phys. Status Solidi, 7* (1964) 937.
12 H. Schultz, *Mater. Sci. Eng., 3* (1968 - 1969) 189.
13 J. Nihoul, in A. Seeger, D. Schumacher, W. Schilling and J. Diehl (eds.), *Vacancies and Interstitials in Metals*, North-Holland, Amsterdam, 1970, p. 839.
14 P. Moser, in R. R. Hasiguti and N. Mikoshiba (eds.), *Internal Friction and Ultrasonic Attenuation in Solids*, University of Tokyo Press, Tokyo, 1977, p. 63.
15 H. Schultz, in R. de Batist, J. Nihoul and R. Stals (eds.), *Defects in Refractory Metals*, S.C.K.–C.E.N., Mol, 1972, p. 383.
16 A. Seeger, in M. T. Robinson and F. W. Young, Jr. (eds.), *Proc. Conf. on the Fundamental Aspects of Radiation Damage in Metals*, Vol. 1, in *ERDA Rep. CONF-751006*, 1976, p. 493, U.S. Energy Research and Development Administration.
17 B. Šesták and A. Seeger, *Z. Metallkd., 69* (1978) 195, 355, 425.
18 H. A. Peretti and M. A. Mondino, *Scr. Metall., 10* (1976) 793.
19 K. Faber, J. Schweikhardt and H. Schultz, *Scr. Metall., 8* (1974) 713.
20 E. Fromm and H. Jehn, *Vacuum, 19* (1969) 191.
21 G. Hörz, *Metall. Trans., 3* (1972) 3069.
22 H. A. Peretti, *Internal Rep. 1971/17*, Centro Atõmico Bariloche, Bariloche, Argentina.
23 J. Schweikhardt, *Dr. rer. nat. thesis*, University of Stuttgart, 1977.
24 F. Dausinger, J. Fuss, J. Schweikhardt and H. Schultz, *J. Nucl. Mater., 69 - 70* (1978) 689.
25 W. Frank, *Phys. Status Solidi B, 72* (1975) 265.
26 K. Maier, H. Metz, D. Herlach, H.-E. Schaefer and A. Seeger, *Phys. Rev. Lett., 39* (1977) 484.
27 M. A. Mondino and A. Seeger, *Scr. Metall., 11* (1977) 817.
28 K. Maier, M. Peo, B. Saile, H.-E. Schaefer and A. Seeger, *Philos. Mag., 40* (1979) 701.
29 K. Sonnenberg, W. Schilling, K. Mika and K. Dettmann, *Radiat. Eff., 16* (1972) 65.
30 W. Frank and A. Seeger, *Radiat. Eff., 31* (1976) 7.
31 A. Seeger and W. Frank, *Radiat. Eff., 31* (1976) 17.
32 G. Lück and R. Sizmann, *Phys. Status Solidi, 5* (1964) 507.
33 G. Lück and R. Sizmann, *Phys. Status Solidi, 6* (1964) 263.
34 K. Urban and A. Seeger, *Philos. Mag., 30* (1974) 1395.
35 L. J. Cuddy, *Acta Metall., 16* (1968) 23.
36 H. A. Peretti and M. Balanzat, unpublished, 1977.
37 P. Jung and W. Schilling, *Phys. Rev. B, 5* (1972) 2046.
38 H. Yoshinaga, *Phys. Status Solidi, 18* (1966) 625.
39 R. Bullough and R. C. Newman, *Proc. R. Soc. London, Ser. A, 266* (1962) 209.
40 H. Kimura, in M. Doyama and Sh. Yoshida (eds.), *Progress in the Study of Point Defects*, University of Tokyo Press, Tokyo, 1977, p. 119.
41 G. Hettich, H. Mehrer and K. Maier, *Scr. Metall., 11* (1977) 795.
42 H.-E. Schaefer, K. Maier, M. Weller, D. Herlach, A. Seeger and J. Diehl, *Scr. Metall., 11* (1977) 803.
43 J. Diehl, U. Merbold and M. Weller, *Scr. Metall., 11* (1977) 811.
44 M. Kaneko, N. Okumura and T. Sugeno, *Scr. Metall., 3* (1969) 849.
45 C. Minier-Cassayre, *Thèse*, Université de Grenoble, 1965.
46 G. Burger, K. Isebeck, R. Kerler, J. Völkl, H. Wenzl, H. H. Kuhlmann and H. Schultz, *Phys. Lett., 20* (1966) 470.
47 P. Moser, *Mem. Sci. Rev. Metall., 63* (1966) 1.
48 W. Decker, J. Diehl, A. Dunlop, W. Frank, H. Kronmüller, W. Mensch, H. E. Schaefer, B. Schwendemann, A. Seeger, H. P. Stark, F. Walz and M. Weller, *Phys. Status Solidi A, 52* (1979) 239.
49 H. Schultz, *Scr. Metall., 8* (1974) 721.
50 C. P. Flynn, *Point Defects and Diffusion*, Clarendon, Oxford, 1972.

APPENDIX A

The relationship of eqn. (1) to the theory of epidemiology

The spreading and threshold behaviour of epidemic diseases in a population is well described by

$$\frac{dS}{dt} = -\alpha SI$$
$$\frac{dI}{dt} = \alpha SI - \beta I \qquad \text{(A1)}$$

where S denotes the number of individuals susceptible to an epidemic and I the number of infectious individuals. α and β are time-independent parameters characteristic for the epidemic [A1]. Equations (A1) become identical with eqns. (1) if $S = -C_V$ and $I = C_I$. The method of solution developed in Section 4.2 may thus be adapted to eqns. (A1).

A1 M. Braun, *Differential Equations and Their Applications (Applied Mathematical Sciences*, Vol. 15), Springer, Berlin, 2nd edn., 1978.